Jordan Journal of Dentistry, Volume **3**, No. **3**, **2026**
DOI: https://doi.org/10.14525/JJD.v3i3.03

Jordan Journal of Dentistry

https://jjd.just.edu.jo

Influence of Alveolar Bone Morphology and Density on Visibility of the Mandibular Canal in Dentate versus Edentulous Mandibles: A Cross-sectional CBCT Study

Malik Hudieb[1], Elham AlQaffaf [2], Hisham Al Shorman[3]

1 Department of Preventive Dentistry, Jordan University of Science and Technology, Irbid, Jordan.
2 Al-Razi University, Sanaa, Yemen.
3 Department of Preventive Dentistry, Zarqa, Jordan.

ARTICLE INFO

Article History:
Received: 25/9/2025
Accepted: 27/12/2025

Correspondence:
Malik Hudieb,
Faculty of Dentistry, Jordan University of Science and Technology, Irbid, Jordan.
mihudieb@just.edu.jo

ABSTRACT

Objectives: This study aims to investigate the influence of alveolar bone morphology and density on mandibular canal (MC) visibility and mental foramen (MF) position in dentate versus edentulous posterior mandibles.

Materials and Methods: Archival CBCT scans from 148 adults (mean age 43.4 ± 16.2 years) were analyzed: 82 dentate and 66 edentulous cases. MC visibility at the first molar site was scored (0–3 scale) on panoramic and parasagittal views. Bone morphology was classified using a modified system integrating prior schemes (Types A-F), density per Lekholm and Zarb (D1-D4), and MF position measured relative to alveolar crest and inferior border. Statistical analyses included Chi-square, t-tests, and Kappa for reliability ($P < 0.05$).

Results: Edentulous mandibles showed significantly higher MC visibility on parasagittal views, with 53.0% of cases having a completely visible canal compared to 29.3% in dentate mandibles ($P < 0.05$); a similar, but non-significant, trend was observed on panoramic views ($P = 0.051$). Morphology distributions differed at MF ($P = 0.032$) and premolar ($P = 0.037$) sites, with posterior Types A/B (lingual concavity/inclination; 65.6% at molars) being predominant. An additional morphology pattern (Type D: narrow base, wide crest), not captured by prior classifications, was observed in 6%-13% of cases. Edentulous cases exhibited denser bone (higher D1; $P < 0.05$). In stratified analysis, MC visibility is associated with morphology in dentate patients ($P < 0.05$), but with bone density in edentulous patients ($P < 0.05$).

Conclusions: Edentulous mandibles showed higher MC visibility compared with dentate mandibles, while the MF position remained stable relative to the inferior border. Bone morphology was highly variable in the posterior region. These findings, including the identification of a new morphological variant (Type D), underscore CBCT's critical role in mitigating risks of inferior alveolar nerve injury and lateral perforation, supporting the development of population-specific classifications for precise implant planning.

Keywords: CBCT, Mandibular canal, Mental foramen, Alveolar bone, Dental implants, Edentulous jaw.

1. Introduction

Dental implant treatment has become a cornerstone of modern dentistry, offering a predictable and reliable solution for rehabilitating partially and fully edentulous patients, with well-documented long-term survival and success rates (1). For diverse clinical scenarios, implant placement protocol encompasses a flexible range from immediate placement following tooth extraction to early placement and conventional delayed placement in healed edentulous ridges. While immediate placement is

often preferred to preserve bone and reduce treatment time, conventional placement suits cases with healed significant bone remodeling. However, all protocols necessitate meticulous preoperative planning to ensure patient safety and long-term success for optimal outcomes. The choice of protocol depends on patient-specific factors, including bone quality and anatomical constraints, particularly in the posterior mandible where risks are elevated (2).

Posterior mandibular region represents a critical region, where local anatomy intersects with adjacent vital structures to represent a challenging area for implant placement. The most significant risks include injury to the neurovascular bundle within the mandibular canal (MC), which can lead to temporary or permanent neurosensory dysfunction, and perforation of the thin lingual cortical plate, which can result in life-threatening hemorrhage or infection (2,3). The incidence of iatrogenic inferior alveolar nerve injury (IANI) related to implant surgery could have a profound and lasting negative impact on a patient's quality of life (3).

Consequently, advanced radiographic evaluation has become the standard of care for preoperative assessment. While two-dimensional radiographs have been conventionally used, they are limited by geometric distortion, magnification, and anatomical superimposition, which can obscure critical structures (4). Cone-beam computed tomography (CBCT) has emerged as the imaging modality of choice, providing high-resolution, three-dimensional, sub-millimeter accurate images with a relatively lower radiation dose compared to medical CT (5). CBCT enables the precise evaluation of bone volume, the course of the MC, and the position of the mental foramen (MF), thereby significantly enhancing surgical safety and planning. The CBCT assessment focuses on two critical and interrelated aspects: bone morphology and bone density.

The mandibular cross-sectional morphology, particularly in the posterior region, is highly variable. The presence of lingual concavities or undercuts, often associated with the submandibular and sublingual fossae, significantly increases the risk of lingual plate perforation during osteotomy preparation (6,3). To categorize these variations, several classification systems have been introduced (7,8,6), yet their applicability across different populations is still to be fully validated. Similarly, bone density, most commonly classified according to Lekholm and Zarb (9), is a key determinant for primary implant stability and long-term osseointegration (9).

A crucial component of the CBCT evaluation is the assessment of the visibility of the MC. Despite the advantages of CBCT, the clarity of the MC is not constant and can be influenced by the density of the surrounding trabecular bone and the degree of cortication of the canal walls, varying considerably between individuals and even within the same mandible (10,11,12). Furthermore, the transition from a dentate to an edentulous state instigates significant alveolar bone remodeling, altering both bone morphology and bone density (9), which may subsequently affect the radiographic visibility of underlying vital structures. The position of the mental foramen is another critical landmark, and its accurate identification is essential to avoid injury to the mental neurovascular bundle during surgery. However, a clear understanding of how these specific factors -bone density and bone morphology- directly influence the visibility of the MC and the position of the MF remains elusive. While the association between bone density and implant outcomes is well-established, its specific influence on the radiographic clarity of the MC is less clear. Similarly, the relationship between cross-sectional jaw morphology and the ability to identify the MC and MF has not been thoroughly investigated.

Therefore, the aims of this cross-sectional CBCT study were to investigate the impact of alveolar bone morphology and density on the visibility of mandibular canal and mental foramen position in dentate and edentulous posterior mandibular regions. By addressing these objectives, this study seeks to provide clinically relevant, population-specific data to improve the safety, precision, and predictability of implant placement in the posterior mandible.

2. Materials and Methods

The study protocol received approval from the Institutional Review Board (IRB) at Jordan University of Science and Technology. Due to the cross sectional study design and anonymization of data, informed consent was waived, ensuring compliance with ethical standards for patient privacy. CBCT scans were randomly selected from the archival database of the Oral and Maxillofacial Surgery Department at Jordan University of Science and Technology Dental Teaching Center, covering referrals for presurgical assessments

from 2013 to 2017. An initial screening of 815 cases yielded 148 eligible patients (81 females, and 67 males; mean age 43.36 ± 16.15 years; age range is 20-82 years) after applying inclusion and exclusion criteria. Patients were stratified into dentate group (n=82) and edentulous group (n=66) based on the presence or absence of posterior mandibular teeth.

To standardize measurements and avoid statistical dependence from bilateral correlations, this study evaluated only the left posterior mandible. This region was selected, because primary screening indicated a higher prevalence of missing teeth on the left side. Inclusion criteria encompassed: adults aged >18 years who were medically healthy; for dentate patients, mild or no periodontitis with intact first molar and premolar teeth; for edentulous patients, residual alveolar bone height ≥12 mm from the crest to the superior MC border (13) and width ≥3.5 mm (14). Exclusion criteria included: systemic conditions or medications impacting bone quality (e.g. bisphosphonates); pathological lesions (radiolucent or radiopaque) at sites of interest; image artifacts or positioning errors; severe periodontitis, periapical pathology, or metallic restorations on relevant teeth; severe alveolar resorption; prior grafting, fractures, or implants in the region; recent extractions with socket visualization; and pediatric cases (<18 years). All scans were performed by certified radiology technicians using the KODAK 9500 Cone Beam 3D System (Carestream, USA) equipped with a flat-panel detector. The field of view was a cylindrical volume (diameter 9–15 cm; height 18-20 cm), producing isotropic voxels of 0.2–0.3 mm. Patients were positioned standing in centric occlusion during a single 360° rotation. Technical parameters included tube current 10–15 mA, voltage 60–90 kV, and exposure time 10–24 seconds, optimizing image quality while minimizing radiation. Post-acquisition, axial, panoramic, and reformatted parasagittal images were reconstructed with 0.2–0.3 mm slice thickness using CS 3D Imaging Viewer software (version 3.2.9; Carestream Health, Inc.).

Evaluations were conducted by a single examiner (intra-examiner Kappa >0.80) on a standardized Dell PC with a 15-inch LCD monitor. Three sites were demarcated on the left posterior mandible via a vertical line perpendicular to the inferior border: first molar (furcation in dentate; corresponding edentulous site), MF, and first premolar (midpoint in dentate; aligned to opposing dentition or radiographic guide in edentulous). Maximum bone height and width were measured first at each site using the software's digital ruler (0.1 mm precision). MC Visibility: At the first molar site, visibility was scored on panoramic reconstructions (200–600 µm thickness) and parasagittal sections using a 0–3 scale adapted from Waltrick et al. (15): 3 (completely visible, fully corticated contours), 2 (partially visible, partial cortication), 1 (slightly visible, no cortication), 0 (invisible). The parasagittal cursor was traversed mesiodistally for comprehensive assessment.

2.1 Bone Morphology

Parasagittal sections at all sites were classified using a novel modification integrating Quirynen et al. (7), Chan et al. (6), and Watanabe et al. (8): Type A (lingual concavity, rounded buccal wall), Type B (lingual inclination, constant width), Type C (wide base, narrow crest), Type D (narrow base, wide crest; newly identified), Type E (parallel walls), Type F (buccal concavity) (Figures 1 and 2).

2.2 Bone Density

Subjectively graded on parasagittal views per Lekholm and Zarb (9): D1 (homogeneous compact bone), D2 (thick cortical with dense trabeculae), D3 (thin cortical with dense trabeculae), D4 (thin cortical with sparse trabeculae). All density assessments were performed under standardized display settings (consistent window width/level) on the same calibrated monitor to minimize variability in subjective evaluation.

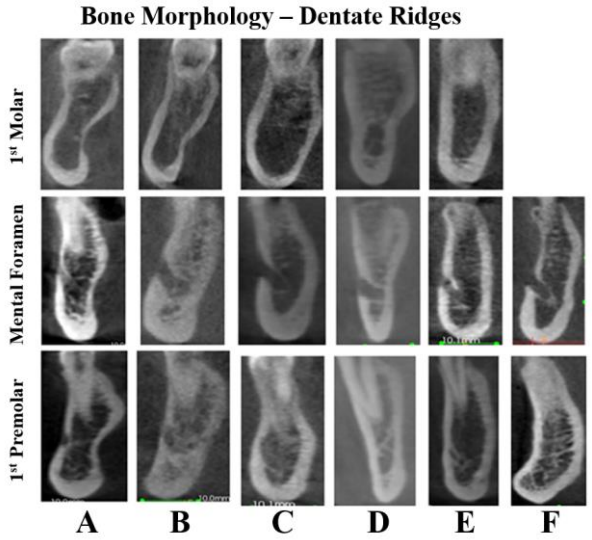

Figure 1: Dentate alveolar bone morphology classification in the parasagittal sections at the first molar, mental foramen and first premolar regions

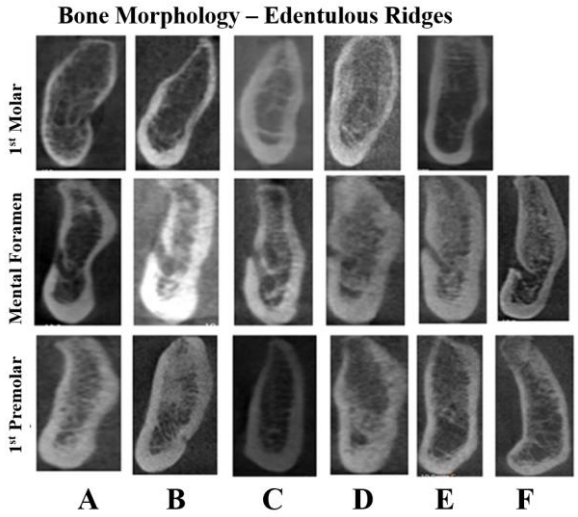

Figure 2: Edentulous alveolar bone morphology classification in the parasagittal sections at the first molar, mental foramen and first premolar regions

2.3 MF Position

At the MF site, superior (MF to crest) and inferior (MF to inferior border) bone heights were measured on panoramic (15-20 µm thickness) and parasagittal views post-maximum dimension determination. Intra-examiner reliability was verified by re-assessing 100 cases after a 1-month interval (Kappa 0.888 for panoramic visibility; 0.809 for parasagittal visibility).

2.4 Statistical Analysis

Data was analyzed with IBM SPSS Statistics (version 22.0; IBM Corp., Armonk, NY, USA). Descriptive statistics included means ± standard deviations for continuous variables and frequencies (percentages) for categorical ones. Normality was tested via Shapiro-Wilk. Group differences (dentate vs. edentulous) for categorical data used Chi-square or Fisher's exact tests (cells <5); continuous data employed independent t-tests (normal) or Mann-Whitney U (non-normal). Associations between morphology/density and MC visibility were assessed via Chi-square. Inter-view agreement (panoramic vs. parasagittal) used Cohen's Kappa. Gender effects were evaluated similarly. Significance was set at $P<0.05$ (two-tailed).

3. Results

A total of 444 para-sagittal scans, from 148 patients (81 females, and 67 males; mean age is 43.36 ± 16.15 years, age range is 20-82 years) were included, with 82 dentate and 66 edentulous individuals. Gender distribution showed no significant differences between groups ($P=0.97$, Chi-square test). The left posterior mandible was analyzed for consistency. Mandibular canal (MC) visibility at the first molar site was assessed on panoramic and parasagittal CBCT views (Figure 3). On panoramic views, no statistically significant differences were found ($P=0.051$, Chi-square test), with edentulous patients exhibiting a higher prevalence of completely visible canals (56.1%) compared to dentate patients. On parasagittal sections, significant differences were found ($P<0.05$, Fisher's exact test), with completely visible canals more frequent in the edentulous group (53.0%) versus dentate group. Intra-examiner agreement was high (Kappa=0.89 for panoramic views, 0.81 for parasagittal views). Agreement between panoramic and parasagittal views was moderate (Kappa=0.72 for dentate group, 0.698 for edentulous) group.

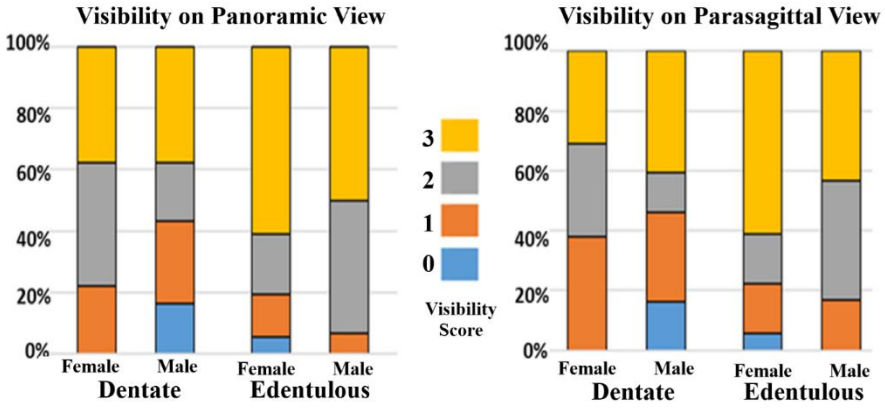

Figure 3: Visibility of mandibular canal on panoramic view (left panel) and parasagittal view (right panel) in dentate and edentulous ridges

Bone height superior and inferior to the mental foramen (MF) was measured on panoramic and parasagittal views (Table 1). Superior bone height was significantly greater in dentate group versus edentulous group on both panoramic (P=0.001, t-test) and parasagittal (P=0.004, t-test) views, reflecting post-extraction remodeling. No significant differences were observed in inferior bone height (P>0.05). Comparing views, superior bone height was significantly higher on panoramic versus parasagittal sections (P<0.001, paired t-test), while inferior height was lower on panoramic views (P<0.001). No significant association was found between MF position and bone morphology (P>0.05, Chi-square test).

Table 1: Comparison of bone height superior and inferior to mental foramen between parasagittal section and panoramic view

	Dentate	Edentulous	Total
	Mean (SD)	**Mean (SD)**	**Mean (SD)**
Parasagittal / Superior	13.4 (2.15)	12.2 (2.65)	12.9 (2.45)
Panoramic / Superior	14.6 (2.25)	13.3 (2.50)	14.0 (2.44)
P-value	**<0.001***	**<0.001***	**<0.001***
Parasagittal / Inferior	12.4 (1.98)	12.5 (1.55)	12.4 (1.79)
Panoramic / Inferior	10.6 (2.10)	10.6 (1.63)	10.6 (1.90)
P-value	**<0.001***	**<0.001***	**<0.001***

* Paired-sample t-test.

Mandibular bone morphology was classified at the first molar, MF, and first premolar sites (Figure 4). At the first molar site, no significant difference in morphology distribution was observed between dentate and edentulous groups (P=0.12, Chi-square test). Type A (lingual concavity, 31.1%) and Type B (lingual inclination, 34.5%) were predominant overall, with Type C (wide base, narrow crest, 2.7%) least common. In dentate patients, Type A (37.8%) was most frequent, while in edentulous patients, Type B (34.8%) prevailed. At the MF site, a significant difference in morphology distribution was noted (P=0.03), with Type E (parallel, 44.6%) and Type C (30.4%) most prevalent overall. At the first premolar site, a significant difference was observed (P=0.04), with Type C (40.5%) and Type E (31.1%) dominant. Type F (buccal concavity) was not observed at first molar site in both dentate and edentulous patients. Type D (narrow base, wide crest) appeared in 12.8% (molar), 9.5% (MF), and 6.1% (premolar) of cases, indicating an additional morphology not fitting prior classifications (7,6,8).

Bone density, assessed per Lekholm and Zarb (9), showed significant differences between dentate and edentulous groups at all sites (P<0.05, Chi-square test). Edentulous patients had a higher prevalence of D1 (homogeneous compact bone) density, while dentate patients predominantly exhibited D2 and D3 (dense trabeculae with thick/thin cortex). No gender-based differences in density distribution were observed (P=0.18).

Analysis of factors associated with MC visibility revealed distinct patterns. In the overall sample, MC visibility was significantly associated with bone morphology (P<0.05, Chi-square test). However, stratified analysis showed that this overall association was driven by the dentate group, where visibility correlated significantly with morphology (P<0.05), but not with density (P>0.05). Conversely, in the edentulous group, visibility was significantly associated with bone density (P<0.05), with higher density (D1) linked to greater visibility, but not with morphology (P>0.05). No gender differences in MC visibility were found (P=0.37 for panoramic group, P=0.40 for parasagittal group).

Maximum bone height ranged from 25.6 ± 3.03 mm (molar) to 29.3 ± 2.8 mm (premolar), and width from 12.0 ± 1.9 mm (premolar/MF) to 13.7 ± 1.9 mm (molar). Males exhibited significantly greater heights and widths than females at all sites (P<0.05, Mann-Whitney U test), except molar width (P=0.06). Dentate patients had greater heights than edentulous patients, particularly at the premolar site (P<0.05).

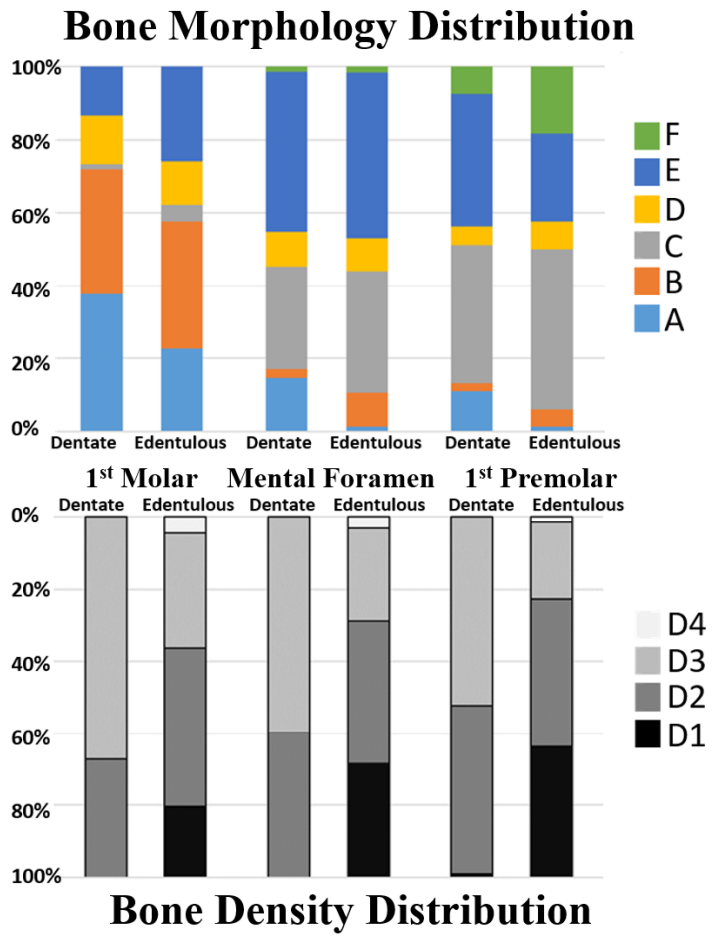

Figure 4: Distribution of alveolar bone morphology classification (upper panel) and bone density (lower panel) in dentate and edentulous

4. Discussion

This cross-sectional CBCT study provides new insights into how the dentate status influences key radiographic and anatomical parameters for implant planning. The principal findings indicate that edentulism is associated with increased bone density and enhanced visibility of the mandibular canal, while revealing significant site-specific variations in bone morphology within the posterior mandible.

Key outcomes included significantly higher MC visibility in edentulous mandibles on parasagittal sections ($P<0.05$), with a non-significant trend on panoramic views ($P=0.051$). The position of the MF relative to the inferior border remained stable between groups. Bone morphology distributions differed significantly at the MF and premolar sites, with Types A and B being predominant in the molar region. A novel morphology pattern (Type D: narrow base, wide crest), not described in existing classifications, was identified. Bone density was significantly higher in edentulous ridges (more D1). Notably, the factors associated with MC visibility differed by dentate status: morphology was the key correlate in dentate patients, while density was the primary factor in edentulous patients.

These findings suggest that the higher MC visibility in edentulous mandibles likely results from alveolar remodeling that reduces trabecular complexity and increases cortical density, facilitating clearer radiographic delineation of the canal. The lack of association between MF position and morphology suggests that MF location is relatively stable despite morphological variations, possibly anchored by neurovascular anatomy rather than by ridge shape. The posterior predominance of Types A and B underscores higher lingual perforation risks in molar regions, while anterior shifts to Types C and E reflect progressive ridge convergence.

The observation of Type D highlights potential population-specific variations, emphasizing the need for tailored morphological assessments. Density differences

imply that tooth loss promotes cortical thickening, potentially improving implant stability, but complicating canal visualization in dentate cases due to root-induced artifacts. Gender and dimensional differences align with known sexual dimorphism in mandibular anatomy, with dentate preservation maintaining greater heights. Relating these to prior studies, the higher MC visibility in edentulous mandibles contrasts with Oliveira-Santos et al. (16) and Nemati et al. (17), who reported no differences between dentate and edentulous groups across multiple sites. This discrepancy may arise from our focus on the first molar region, where remodeling is pronounced, versus their multi-site evaluations. Similarly, Naitoh et al. (11) found a positive correlation between cancellous density and MC depiction, mirroring our edentulous-density association, but we extend this by demonstrating group-specific influences: morphology-driven in dentate group (possibly due to variable undercuts obscuring canal walls) and density-driven in edentulous group (higher D1 aiding cortication visibility).

For bone morphology, our molar prevalence of Types A and B (equivalent to U/undercut in Chan et al. (6)) aligns with Yoon et al. (18) (60% concave in molars) and Huang et al. (19) (56.2% U-type in dentate), but differs from Watanabe et al. (8), where Type C (round) dominated molars, potentially due to ethnic variations (Japanese vs. Jordanian). Anteriorly, our Type C/E dominance echoes Quirynen et al. (7) (69.5% Type III/convergent in premolars) and Nickenig et al. (20) (60.9% parallel in edentulous premolars), supporting a posterior-anterior gradient in concavity reduction. The newly identified Type D, absent in prior systems, suggests evolutionary or dietary influences in Middle Eastern populations, warranting validation. MF findings concur with Fishel et al. (21) and Panjnoush et al. (22) on superior height reduction post-extraction, but our view comparison (panoramic overestimation) highlights CBCT's superiority over 2D imaging (4). Jaw dimensions are consistent with Watanabe et al. (8) (heights 26–29 mm, widths 12-14 mm) and male-female disparities per Herranz-Aparicio et al. (23). Alternative explanations for these findings include methodological factors: subjective density assessment via Lekholm and Zarb (9) may be influenced by CBCT's gray value limitations (24), potentially overestimating D1 in edentulous mandibles due to reduced scattering from absent roots. Visibility differences also could stem from voxel size or field-of-view variations affecting resolution (15), though our protocol (0.2-0.3 mm voxels) minimized this effect.

The absence of Type F (buccal concavity) at the first molar site in both dentate patients and edentulous patients aligns with the anatomical characteristics of the posterior mandible where the external oblique ridge runs along the buccal surface resulting in generally convex, rounded, or ridged surface rather than concave surface.

Morphological shifts might reflect time since edentulism -untracked here- causing progressive resorption (25), or ethnic bone patterns, as Agthong et al. (26) noted racial MF variations. The lack of MF-morphology link could indicate compensatory remodeling preserving neurovascular integrity, rather than direct causation. Clinically, these results advocate for CBCT as a standard for posterior mandibular implants, particularly in molars where Types A/B elevate lingual perforation risks (64.7% vs. 11.75% in premolars), necessitating lingual flap reflection and angled drilling (27,6). Higher edentulous visibility supports delayed placement safety, but dentate cases require multi-view confirmation to mitigate root artifacts. The newly identified Type D classification enhances preoperative planning in diverse populations, reducing IANI incidence (28)). Parasagittal superiority for MF positioning (avoiding panoramic distortion) prevents mental nerve injury (3). Overall, findings promote population-specific protocols, improving osseointegration (9) and quality of life (29).

Limitations include the sample size of 148 patients (444 sites) which might be adequate for the primary comparisons; however, the relatively low prevalence of the additional Type D morphology (6%-13%) limits precision in subgroup estimates and generalizability, indicating the need for larger future multi-center studies. Also, the cross sectional study design omitted edentulism duration, which might influence remodeling (9). Subjective density evaluation lacks Hounsfield unit quantification, though CBCT's utility is supported (30). Single-examiner assessment, despite high reliability (Kappa>0.80), risks bias; inter-observer validation would strengthen the results. Only three sites were evaluated; comprehensive mandibular mapping could reveal broader patterns.

5. Conclusions

In conclusion, this cross-sectional study

demonstrates that edentulism is associated with higher bone density and enhanced MC visibility compared to dentate ridges. The study also identifies a distinct morphological pattern (Type D) not captured by existing classifications. These insights emphasize the critical role of CBCT in avoiding implant-related risks and support the refinement of population-specific morphological assessments for accurate planning and safer posterior mandibular implant placement.

Conflict of Interests

The authors declare that they have no competing interests regarding the authorship or publication of this article.

Funding Information

This study is funded by the Deanship of Scientific Research – Jordan University of Science and Technology, Irbid, Jordan.

References

1. Buser D, Janner SFM, Wittneben JG, Brägger U, Ramseier CA, et al. 10-year survival and success rates of 511 titanium implants with a sandblasted and acid-etched surface: A study in 303 partially edentulous patients. Clin Implant Dent Relat Res. 2012;14:839-851.
2. Du Toit J, Gluckman H, Gamil R, Renton T. Implant injury case series and review of the literature part 1: Inferior alveolar nerve injury. J Oral Implantol. 2015;41:e144-e151.
3. Alhassani AA, AlGhamdi AST. Inferior alveolar nerve injury in implant dentistry: Diagnosis, causes, prevention, and management. J Oral Implantol. 2010;36:401-407.
4. Lindh C, Petersson A. Radiographic examination for location of the mandibular canal: a comparison of panoramic radiography and conventional tomography. Int J Oral Maxillofac Surg. 1989;18:306-309.
5. Lofthag-Hansen S, Gröndahl K, Ekestubbe A. Cone-beam CT for preoperative implant planning in the posterior mandible: Visibility of anatomic landmarks. Clin Implant Dent Relat Res. 2009;11:246-255.
6. Chan HL, Benavides E, Yeh CY, Hayashi K, Wang HL, et al. Risk assessment of lingual plate perforation in posterior mandibular region using cone-beam computed tomography: A study of 181 consecutive patients. J Periodontol. 2011;82:1608-1616.
7. Quirynen M, van Assche N, Botticelli D, Berglundh T. How does the timing of implant placement to extraction affect outcome? Int J Oral Maxillofac Implants. 2003;22 Suppl:203-223.
8. Watanabe H, Mohammad Abdul M, Kurabayashi T, Aoki H. Mandible size and morphology determined with CT on a premise of dental implant operation. Surg Radiol Anat. 2010;32:343-349.
9. Lekholm U, Zarb GA. Patient selection and preparation. In: Brånemark PI, Zarb GA, Albrektsson T, eds. Tissue-Integrated Prostheses: Osseointegration in Clinical Dentistry. Chicago: Quintessence; 1985:199-209.
10. Angelopoulos C, Thomas SL, Hechler S, Parissis N, Hlavacek M, et al. Comparison between digital panoramic radiography and cone-beam computed tomography for the identification of the mandibular canal as part of presurgical dental implant assessment. J Oral Maxillofac Surg. 2008;66:2130-2135.
11. Naitoh M, Katsumata A, Kubota Y, Hayashi M, Ariji E, et al. Assessment of bone density in the posterior mandible for dental implant planning using cone-beam CT. Int J Oral Maxillofac Implants. 2009;24:494-500.
12. Shokri A, Shakibaei Z, Langaroodi AJ, Safaei M. Evaluation of the mandibular canal visibility on cone-beam computed tomography images of the mandible. J Craniofac Surg. 2014;25:e273-e277.
13. Sammartino G, Marenzi G, Citarella R, Ciccarelli R, Wang HL, et al. Analysis of the mandibular canal course: A cone-beam computed tomography study. Clin Oral Implants Res. 2008;19:1213-1218.
14. Chiapasco M, Zaniboni M, Boisco M. Augmentation procedures for the rehabilitation of deficient edentulous ridges with dental implants. Clin Oral Implants Res. 1999;10:191–201.
15. Waltrick KB, Nunes MJ, Guedes OA, Guedes FR, Mazzi-Chaves JF, et al. Radiographic evaluation of mandibular canal visibility using cone beam computed tomography. J Oral Maxillofac Surg. 2013;71:e60-e61.
16. Oliveira-Santos C, Capelozza ALA, Dezzoti MSG, Fischer CM, Poleti ML, et al. Visibility of the mandibular canal on CBCT cross-sectional images. J Appl Oral Sci. 2011;19:240-243.
17. Nemati S, Dalili Kajan Z, Saberi BV, Zareh S, Rasoolzadeh A, et al. Comparison of mandibular canal

visibility on panoramic and cross-sectional CBCT images in patients with different dental status. J Dent Res Dent Clin Dent Prospects. 2016;10:37-43.
18. Yoon TY, Kim JJ, Lee SJ, Kim MK, Lim HJ, et al. Anatomical variations of the mandibular canal and mental foramen in cone beam CT: A study. J Korean Acad Conserv Dent. 2017;42:123-130.
19. Huang H, Zhang G, Xiao Q, Liu Z, Zhang Z, et al. Assessment of mandibular posterior lingual concavity using cone beam computed tomography. Int J Clin Exp Med. 2015;8:12705-12712.
20. Nickenig HJ, Wichmann M, Eitner S, Zöller JE, Kreppel M, et al. Lingual concavity in the posterior mandible: A study using cone beam CT. Clin Oral Implants Res. 2015;26:870-875.
21. Fishel D, Buchner A, Hershkowith A. Roentgenologic study of the mental foramen. Oral Surg Oral Med Oral Pathol. 1976;41:682-686.
22. Panjnoush M, Rabiee S, Shokri A, Norouzi M. Evaluation of mandibular canal and mental foramen using cone beam computed tomography. J Dent (Tehran). 2016;34:1-8.
23. Herranz-Aparicio J, Marques J, Almendros-Marqués N, Gay-Escoda C. Study of the bone morphology in the posterior mandibular region. Evaluation of the prevalence of the lingual concavity using CBCT. Med Oral Patol Oral Cir Bucal. 2016;21:e731-e736.
24. Varshowsaz M, Goorang S, Ehsani S, Azizi Z, Rahimian S, et al. Comparison of tissue density in Hounsfield units in computed tomography and cone beam computed tomography. J Dent (Tehran). 2016;13:108-115.
25. Pietrokovski J. The bony residual ridge in man. J Prosthet Dent. 1975;34:456-462.
26. Agthong S, Huanmanop T, Chentanez V. Anatomical variations of the supraorbital, infraorbital, and mental foramina related to gender and side. J Oral Maxillofac Surg. 2005;63:800-804.
27. Greenstein G, Cavallaro J, Romanos G, Tarnow D. Clinical recommendations for avoiding and managing surgical complications associated with implant dentistry. J Periodontol. 2008;79:1317-1329.
28. Bartling R, Freeman K, Kraut RA. The incidence of altered sensation of the mental nerve after mandibular implant placement. J Oral Maxillofac Surg. 1999;57:1408-1412.
29. Abarca M, van Steenberghe D, Malevez C, De Ridder J, Jacobs R, et al. Neurosensory disturbances after immediate loading of implants in the anterior mandible: An initial questionnaire approach followed by a psychophysical assessment. Clin Oral Investig. 2006;10:269-277.
30. Parsa A, Ibrahim N, Hassan B, van der Stelt P, Wismeijer D, et al. Reliability of voxel grey values in cone beam computed tomography for preoperative implant planning. Int J Oral Maxillofac Implants. 2015;30:511-517.